Fish and Shellfish Immunology 88 (2019) 528–539

Contents lists available at ScienceDirect

Fish and Shellfish Immunology

journal homepage: www.elsevier.com/locate/fsi

Full length article

Insights into the molecular basis of immunosuppression and increasing pathogen infection severity of ammonia toxicity by transcriptome analysis in pacific white shrimp *Litopenaeus vannamei*

Xia Lu[a,b], Sheng Luan[a,b], Ping Dai[a,b], Kun Luo[a,b], Baolong Chen[a,b], Baoxiang Cao[a,b], Li Sun[a,c], Yunjun Yan[a,d], Jie Kong[a,b,*]

[a] Key Laboratory of Sustainable Utilization of Marine Fisheries Resources, Ministry of Agriculture, Yellow Sea Fisheries Research Institute, Chinese Academy of Fishery Sciences, Qingdao, 266071, China
[b] Laboratory for Marine Fisheries Science and Food Production Processes, Qingdao National Laboratory for Marine Science and Technology, Qingdao, 266071, China
[c] College of Fisheries and Life Science, Shanghai Ocean University, Shanghai, 201306, China
[d] Wuxi Fisheries College, Nanjing Agricultural University, Wuxi, 214081, China

ARTICLE INFO

Keywords:
Immunosuppression
Ammonia toxicity
WSSV
Transcriptome analysis
Litopenaeus vannamei

ABSTRACT

The high concentration of ammonia resulting from intensive culture system and environmental pollution could cause disease occurrence in shrimp, but little information is available on its molecular mechanisms. In this study, we performed comparative transcriptome analysis among WSSV-infected shrimp under ammonia stress (LAV), WSSV-infected shrimp under normal water (LV), and normal shrimp under ammonia stress (LA) groups to identify the key genes and pathways involved in immunosuppression and increasing pathogen infection severity caused by ammonia toxicity in *Litopenaeus vannamei*. Totally, 526 significantly differential expressed genes (DEGs) were identified in LAV group compared to LV and LA groups, among which 270 genes were lost expressed and 67 genes uniquely expressed in the LAV group. According to the public functional reports for the annotated DEGs, they potentially involved in the following functions: (1) accelerating pathogen adhesion, invasion and multiplication; (2) reducing the ability for pathogen defense and immune response; (3) inhibiting positive regulation of apoptotic and antioxidant defense for host homeostasis; (4) inhibiting transcription and protein transport; (5) and increasing protein methylation and ubiquitination, etc. A total of 13 pathways were obtained mainly involving in this process, which mainly led to the following changes: (1) increasing the immunosuppression, anemia, endocrine dysfunction, neurotoxic effect and neuroinvasion, atherosclerosis and thrombogenesis, blood-brain barrier penetration, thyroid disorder, necrosis, inflammation, and circadian disturbance; (2) reducing the ability of vascular remodeling, angiogenesis, cell survival, migration, apoptosis, and lymph transferred to blood stream; (3) leading to cell hypertrophy, cellular shape changes, and mesangial matrix expansion. The present results firstly supplied molecular mechanisms for the ammonia toxicity inhibiting the immune system and increasing pathogen infection severity in shrimp, which is a prerequisite for better understanding the pathogenesis caused by ammonia toxicity.

1. Introduction

The Pacific white shrimp, *Litopenaeus vannamei*, provides approximately 52% of the total penaeid shrimp output in the world [1]. However, its production is badly reduced by diseases recently, such as the acute hepatopancreas necrosis syndrome (AHPNS) and the white spot syndrome virus (WSSV), etc. In addition, the deteriorated aquaculture environments and intensive culture systems often result in degradation of the culture water, and the toxicity from the degraded culture water factors is playing an important role in the high mortality of shrimp by increasing pathogen infection severity [2,3].

Among the degraded water factors, high concentration of ammonia is the commonest toxic factor to shrimp. Many studies have revealed that ammonia toxicity in the water could cause disease occurrence by increasing pathogen infection severity in aquatic species. For example, Li et al. [4] have revealed that ammonia has the biggest effects on the severity grade of pathogen infection, and the infection severity grade rises obviously when ammonia level rises. Liu et al. [5] have studied the

* Corresponding author. 106 Nanjing Road, Qingdao, 266071, China.
E-mail address: aquagene@163.com (J. Kong).

https://doi.org/10.1016/j.fsi.2019.03.026
Received 1 January 2019; Received in revised form 9 March 2019; Accepted 12 March 2019
Available online 16 March 2019

effect of ammonia on the immune response of *L. vannamei* and its susceptibility to *Vibrio alginolyticus*. In their study, the growth of *V. alginolyticus* was not affected by ammonia concentration within the range of 0–20 mg/L and there was no significant difference in cumulative mortality for shrimp incubated in this range of ammonia concentration after 120 h of challenge; however, the mortality of *Vibrio*-infected shrimp under ammonia stress was significantly higher than the *Vibrio*-infected shrimp under normal water and control group after 48–168 h, and the mortality increased directly with ammonia concentration and expose time [5]. In addition, we also found the consistent results on the effect of ammonia toxicity on the immune response of *L. vannamei* and its susceptibility to virus in our previous study [6]. In our previous study, the mortality of WSSV-infected shrimp under ammonia stress was significantly higher than that of the WSSV-infected shrimp under normal water and control group after 120–144 h of challenge, and the ammonia-tolerant shrimp also have high resistance to WSSV compared to the ammonia-sensitive shrimp [6]. In mollusk, Cheng et al. [7] investigated the effect of ammonia toxicity on the immune response of Taiwan abalone *Haliotis diversicolor supertexta* and its susceptibility to *V. parahaemolyticus*, and they concluded that ammonia stress caused a depression in immune parameters and an increase in mortality of *H. diversicolor supertexta* after *V. parahaemolyticus* infection. The same situation also has been detected in fish, such as rainbow trout [8].

However, how the ammonia toxicity inhibits the immune defense system and increases pathogen infection severity in not clear. In recent years, the complicated, fickle, and deteriorated aquaculture environments is inevitable, which usually cause high concentration of ammonia that have grievous harm in shrimp aquaculture. Consequently, it is vital to understand the molecular mechanism of disease occurrence caused by ammonia toxicity for seeking possibilities of culturing shrimp that efficiently resist the pathogens, which might be an alternative method to reduce mortality and infectious diseases. To study the changes of gene expression and metabolic pathways respond to pathogen infection under ammonia stress is a priority for understanding of the molecular mechanism in the non-model species with rare genomic resources. Along with the recent development in next-generation sequencing (NGS) technologies, whole-transcriptome shotgun sequencing, also known as RNA sequencing (RNA-seq), is often used to capture and annotate the transcriptome for understanding the molecular mechanism of a specific physiological process. RNA-seq technology could detect nearly all of the genes and pathways involved in the corresponding physiological function with high sensitivity [9–11], which has been widely applied to the stress and infection studies in shrimp [12–14].

In order to explain how the ammonia toxicity inhibits the immune defense system and increases pathogen infection severity, in the present study, we used RNA-Seq technology to identify the genes and pathways that involved in disease occurrence from ammonia toxicity in *L. vannamei*. This study represents the first investigation of the molecular mechanism of disease occurrence caused by ammonia toxicity in aquaculture.

2. Materials and methods

2.1. Shrimps and challenge experiment

The L. *vannamei* used in this study were bred at the Mariculture Genetic Breeding Center of the Chinese Ministry of Agriculture (Qingdao, China). Before the challenge experiment, a total of 60 shrimps (with average body weight of 3.68 ± 0.05 g) were acclimated for one week at the aquaculture workshop in Yellow Sea Fisheries Research Institute (YSFRI), Chinese Academy of Fisheries Research Institute (CAFS). During the period of acclimation, the shrimps were feeding a commercial diet four times per day, which containing 12% moisture, 44% crude protein and 16% crude ash. In addition, 80% of their water was exchanged every day to maintain the ammonia concentration at normal level (less than 0.02 mg/L). The holding water conditions were as follows: salinity at 30‰, pH at 7.9 ± 0.1, and temperature at 27 ± 0.5 °C. After the acclimation, the individuals were randomly equally divided into three groups and performed different treatments as follows: LAV group was cultured under high-concentration ammonia (~10 mg/L) and then infected with WSSV, LV group was cultured under normal-concentration ammonia (< 0.1 mg/L) and infected with WSSV, and LA group was cultured under high-concentration ammonia (~10 mg/L) without WSSV infection.

The WSSV infection was performed as the method described by Shi et al. [15]. Briefly, the frozen muscle tissue from WSSV-infected shrimp was used for WSSV-containing bait. The genomic DNA of the WSSV-containing bait was extracted using the Rapid Genomic DNA Extraction Kit (BioMed Ltd., Beijing, China) according to the protocol provided by the manufacturer, and its WSSV load was quantified by fluorescent real-time PCR with the Premix Ex Taq™ Kit (Takara, Japan) using an ABI 7500 (Applied Biosystems China, Beijing, China). The plasmid PUCm-T/WSSV69 of our laboratory was used as a positive control and standard to establish the qPCR standard curve according to the previous report [16]. Then, the WSSV-containing bait was minced and diluted with the uninfected muscle tissue to the WSSV dose of 10^4 copy/mg tissue. After starving for 24 h, each individual of the two groups was fed the minced and colored WSSV-containing bait (10 mg tissue one shrimp) (Patent number ZL201210107377.8). The ammonia solution was prepared using NH_4Cl (Aldrich, Milwaukee, WI, USA). After challenge, the shrimps were cultured as usual, including feeding shrimp two times a day, and removing feces and leftovers at the bottom of the tanks. During the experiment, 100% of the water of the three groups was exchanged twice per day with ammonia solution (~10 mg/L) and normal water, respectively, to maintain the ammonia concentration level.

According to the previous study, the pre-patent stage of WSSV infection was 2-step WSSV PCR-positive and might persist for months, and at this stage the infected shrimp showed no clinical signs of white spot syndrome [2]. However, transition from pre-patent stage to patent stage that was 1-step WSSV PCR-positive happened within 24–48 h under stressful condition [2]. At the patent stage, positive signals of the virus were detected in the hepatopancreas, lymphoid organs, hemocyte in heart, antennal glands, hart, stomach, epidermis, and muscle by in situ hybridization [2], and all of these tissues locate in cephalothorax. We are more interested in the changes of gene expression and pathways at the initial stage of transition from pre-patent stage to patent stage caused by ammonia stress. So when the shrimps were challenged for 24 h, the cephalothorax of three individuals from each group were separately dissected and frozen immediately in liquid nitrogen, and after that they were stored at −80 °C until RNA extraction, which was completed within one week.

2.2. RNA quantification and qualification

For each group, three individuals were performed RNA extraction separately from the cephalothorax (without eyes, legs and outer coverings) using Trizol Reagent (Qiagen, Hilden, Germany) following with the manufacturer's protocol. After the genomic DNA was cleaned from RNA with RNase free DNase I (Takara, Japan), the RNA degradation and contamination was monitored on 1% agarose gels. After that, the purity, concentration, and integrity of the RNA were checked using NanoPhotometer® spectrophotometer (IMPLEN, CA, USA), Qubit® RNA Assay Kit in Qubit® 2.0 Fluorometer (Life Technologies, CA, USA), and RNA Nano 6000 Assay Kit of the Agilent Bioanalyzer 2100 system (Agilent Technologies, CA, USA), respectively, which also has been described by Huang et al. [17]. According to the checking result, all of the RNA samples are high-quality ($OD_{260/280}$ = 2.0–2.2, $OD_{260/230} \geqq 2.0$, RIN ≧ 8.0, and 28S:18S ≧ 1.0).

2.3. Library preparation and transcriptome sequencing

A total amount of 1.5 μg RNA per sample was used as input material for the RNA sample preparations. The library was constructed using NEBNext® Ultra™ RNA Library Pep Kit for Illumina® (NEB, USA) according to the manufacture's recommendation. Briefly, poly-T oligo-attached magnetic beads were used to purify the mRNA from the total RNA. Fragmentation was carried out using divalent cations under elevated temperature in NEBNext First Stand Synthesis Reaction Buffer (5×). Then, first-strand cDNA was synthetized with the cleaved RNA fragments with M-MuLV Reverse Transcripase (RNase H^-), and the second-strand cDNA was synthetized with RNase H and DNA polymerase I. Remaining overhangs were converted into blunt ends via exonuclease/polymerase activities. NEBNext Adapter with hairpin loop structure were ligated to the synthetized cDNA fragments after adenylation of 3′ ends of DNA fragments for hybridization. In order to select cDNA fragments of preferentially 250–300 bp, the library fragments were purified with AMPure XP system (Beckman Coulter, Beverly, USA). Then 3 μL USER Enzyme (NEB, USA) was used with size-selected, adaptor-ligated cDNA at 37 °C for 15 min followed by 5 min at 95 °C before PCR, and then PCR was performed with Phusion High-Fidelity DNA polymerase, Universal PCR primers and Index (X) primer. At last, PCR products were purified (AMPure XP system) and library quality was assessed on the Agilent Bioanalyzer 2100 system. The clustering of the index-coded samples was performed on a cBot Cluster Generation System using TruSeq PE Cluster Kit v3-cBot-HS (Illumia) according to the manufacturer's instructions, and then the library preparations were sequenced on an Illumina Hiseq platform and paired-end reads were generated.

2.4. De novo transcriptome assembly and gene function annotation

The adapter sequences, low quality reads, and reads with ploy-N were removed from the raw reads, and then the high quality clean reads were used for the downstream analysis. The obtained clean reads were then randomly clipped into overlapping K-mers with default K = 25 for assembly with the Trinity software [18]. The non-redundant sequences were subjected to BLAST searches and annotations against the Swiss-Prot (A manually annotated and reviewed protein sequence database), Nr (NCBI non-redundant protein sequences) and Nt (NCBI non-redundant nucleotide sequences) using BlastX algorithm with an E-value cut-off of 10^{-10}. After that GO (Gene Ontology), KOG/COG (Clusters of Orthologous Groups of proteins), and KO (KEGG Ortholog database) were analyzed with Blast2GO, BlastX 2.2.24+, and BlastX/BlastP 2.2.24 + software, respectively. Pfam (Protein family) available on the web from USA (http://pfam.janelia.org/) was also performed. If the annotation result from the different databases is conflicted, the priority order of alignments for the databases was Nr, Nt, KO, Swiss-Prot, Pfam, GO, and COG.

2.5. Differential expression and cluster analysis

The samples of the present study had biological replicates, so the DEGseq R package (1.20.1) was used to perform a differential expression analysis for LAV, LV, and LA groups, which provides statistical routines for determining differentially expressed genes (DEGs) using a model basing on the negative binomial distribution. Benjaminiand Hochberg's approach was used to adjust the resulting *P* value (q value) for monitoring false discovery rate [19]. The genes with a q value < 0.05 were assigned as significantly differential expression. In addition, a cluster analysis was performed to identify DEGs among LAV, LV and LA groups using an R package of *pheatmap*, according to their relative expression level (log2 (ratios)) between the two groups.

2.6. Enrichment analysis of GO and KEGG

A functional enrichment analysis was performed to identify the DEGs that were significantly enriched in GO terms (with q value < 0.05), which was implemented by GOseq R packages based on Wallenius non-central hyper-genometric distribution [20] to adjust for gene length bias in DEGs. The KEGG pathway is vital for understanding the functions and utilities of the biological system from molecular level information [21], so enrichment analysis also was performed to identify the DEGs that were significantly enriched in KEGG pathways (with p value < 0.05) relative to the whole transcriptome background with the KOBAS software [22].

2.7. Identification of key genes involved in the process

It has been revealed that increased ammonia in the water could inhibit the immune system and increase the susceptibility to pathogens in shrimp, which was very important for the shrimp farming, so identification of differently expressed genes was carried out from the DEGs in the BLASTX alignment results with Nr, Nt, KO, Swiss-Prot, Pfam, GO and KOG databases. The Glycosylphosphatidylinositol (GPI) anchored proteins were detected using the GPI Prediction Server (http://mendel.imp.ac.at/sat/gpi/gpi_server.html) and then removed from the results [23,24]. The DEGs enriched to the significantly changed GO terms and KEGG pathways between LV_AV and LV_V were selected and identified as key genes potentially involved in immunosuppression process of ammonia toxicity. The unigene with maximum E-value was selected as the representative, when several unique transcripts were assigned to the same reference gene.

2.8. Gene expression validation

For validation of the Illumina sequencing data, seven differentially expressed genes were selected to be quantified by real-time PCR with the same six separate RNA samples used for the Illumina sequencing in each group. Their primers were designed using the Primer Premier 5 software (Premier Biosoft International) according to Illumina sequencing data. The details of the primers are displayed in Table 1. The 18S ribosomal RNA gene of *L. vannamei* was selected as an internal control to normalize the expression level; its primers (F: TATACGCTAGTGGA GCTGGAA, R: GGGGAGGTAGTGACGAAAAAT, and Ta: 54 °C) were referenced in the previous study by Zhang et al. [25]. After the mRNA was reverse transcribed into cDNA, real time PCR was performed in an ABI 7900 HT Sequence Detection System (ABI, USA) and all of the samples were performed in triplicate. RT-PCR was carried out in a total volume of 10 μL, containing 5 μL of 2 × SYBR Green PCR buffer, 0.5 μL of each primer (10 μM), 5 ng of cDNA and Milli-Q water added to reach

Table 1
Primers used for real-time PCR of the seven genes.

Genes	Primer name	Sequence (5′-3′)	Tm (°C)
actin 1	Act-F	TCCATCATGAGGTGCGACAT	54
	Act-R	ATACTCCTCCTTGGTGATCCA	
cAMP-dependent protein kinase catalytic subunit	cpkA-F	AGAAGAATGCACGAGAACGA	54
	cpkA-R	GCCATGGGATAGATACTGAGC	
Importin-9	Imp-F	TGAACACACAGCCACTTTTGT	54
	Imp-R	AAGAGATGCTGTTTGGAGCA	
Spz2	Spz2-F	ACAGCCCACCTGACTGTACC	54
	Spz2-R	ATCGCTACTGACGAGGCAAT	
hemolymph clottable protein	CP-F	GTGAGAACCATCAGTGTGGAA	54
	CP-R	TCGTACAATTCGGCCTTGAT	
apoptosis signal-regulating kinase 1	ASK1-F	TCCAGACCATGAGAGCCTACT	54
	ASK1-R	ACACCCAACTGCTCAGCCA	
O-methyltransferase	OMT-F	ACGCCGACAAGACCAACTA	54
	OMT-R	AAGCCATCGCCAATCTTGA	

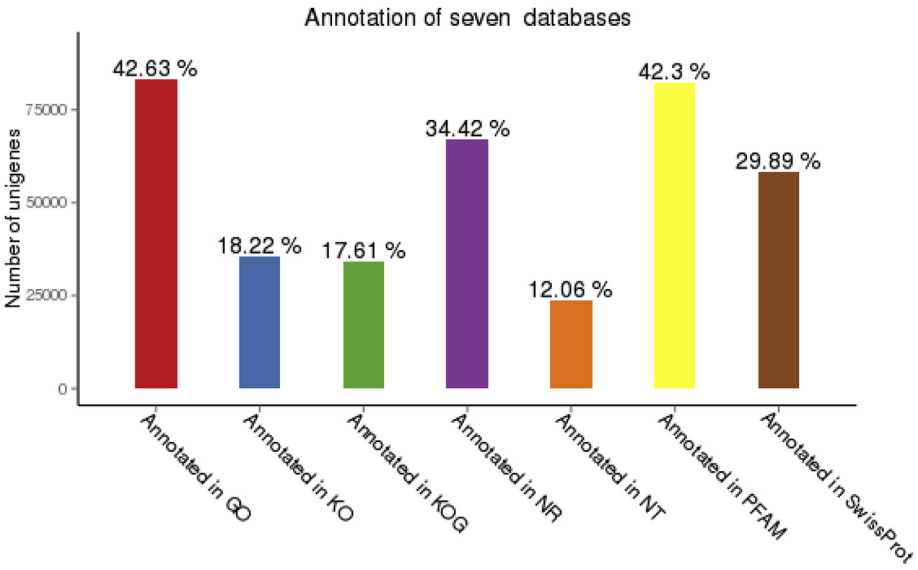

Fig. 1. The distribution of the annotated genes in the 7 public databases.

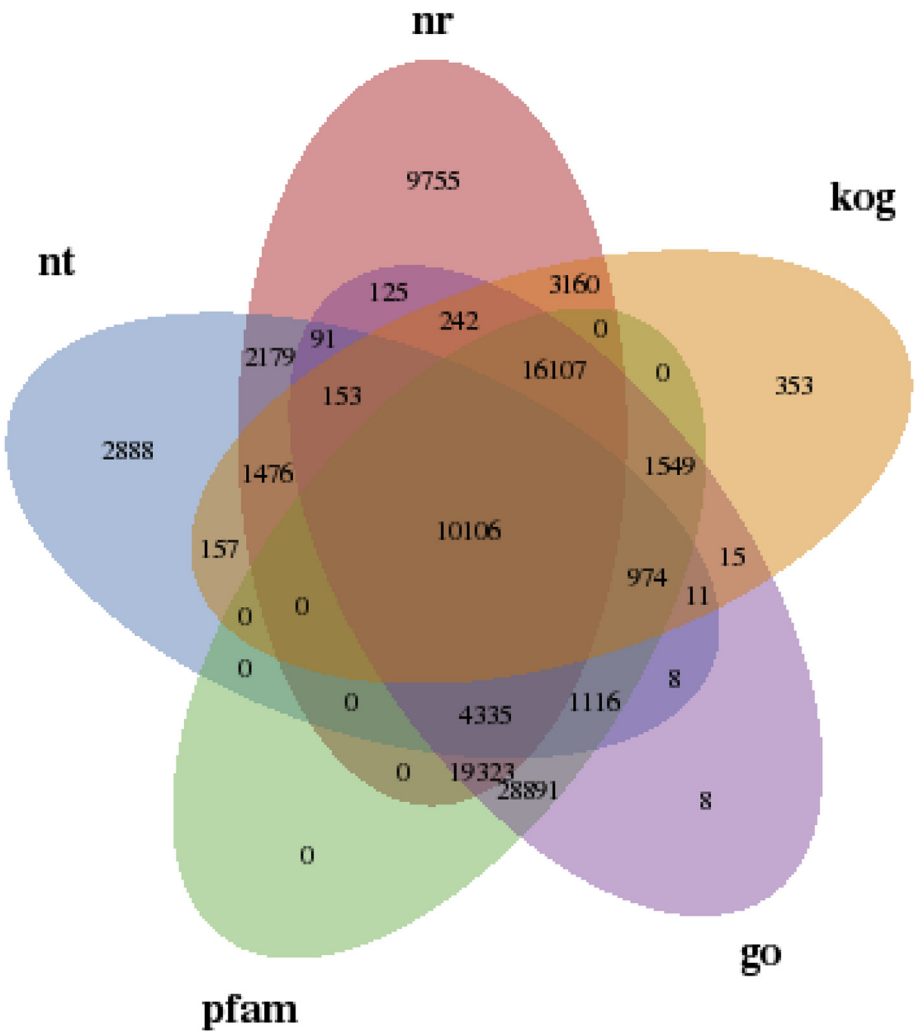

Fig. 2. The Venn diagram in the top five public databases for the annotated genes.

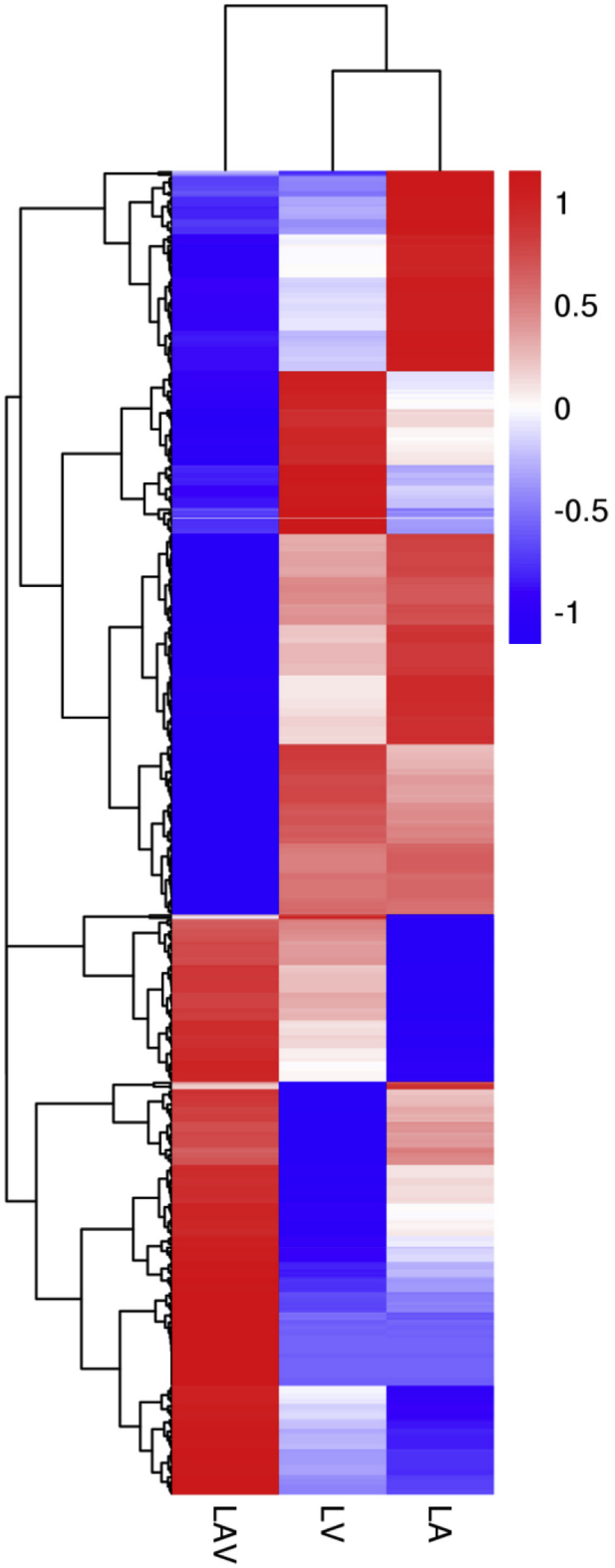

Fig. 3. The hierarchical clustering for the differentially expressed genes between LAV and LV and LA. The red color shows the high expression, and the blue color represents the down expression. The color from red to blue represents the log10 (FPKM + 1) from large to small.

a final volume of 10 μL. The PCR cycling parameters as follows: 50 °C for 2 min, 95 °C for 10 min, followed by 40 cycles of 95 °C for 15 s and 60 °C for 1 min. In order to ensure that only one PCR product was amplified, a dissociation curve analysis was performed for the products at the end of each PCR reaction. The data were analyzed using comparative CT method ($2^{-\Delta\Delta}$ CT method) for the expression level of the genes.

3. Results

3.1. Transcriptome sequencing and assembly

Illumina sequencing totally generated 434, 245, 734 raw reads, which were deposited in the Short Read Archive (SRA) of the National Center for Biotechnology Information (NCBI) with the accession number of https://www.ncbi.nlm.nih.gov/sra/PRJNA507041. The mean values of the Q20% and Q30% are 96.92% and 92.35%, respectively, and the error rate is 0.02%. After removing the adapter sequences, ambiguous nucleotides and low-quality sequences, a total of 424, 956, 014 clean reads were generated through Illumina sequencing. A total of 63.73 G clean bases were generated from the clean reads, and the average percentage of GC content for the clean reads was 49.96%.

The clean bases were performed *de novo* assembly using Trinity software and assembled into 330,348 transcripts with a total length of 276, 945, 177 nucleotides. The length of the transcripts ranged from 201 bp to 31,943 bp with an average length of 838 bp and N50 of 1609. These transcripts were subsequently assembled into 194,790 unigenes that ranged from 201 bp to 31,943 bp with an average length of 1217 bp and N50 of 1983. N50 length is defined as the contig length L for which 50% of all bases in the sequences is in contigs of length less than L. The total length of the unigenes is 237, 120, 622 bp, which covered 85.92% of the length of transcripts.

3.2. Functional annotation of unigenes

After removing the low-quality and short-length sequences, an annotation analysis was performed on the remaining 194,790 non-redundant unigenes by matching sequences against the 7 public databases. The distribution of the annotated genes in the 7 public databases are summarized in Fig. 1. The highest percentage of unigenes was annotated in the GO database (83,054, 42.63%), followed by the Pfam database (82,401, 42.30%) and the Nr database (67,052, 34.42%). The Venn diagram for the annotated genes in the top five public databases (Fig. 2) showed that many genes are simultaneously annotated in different databases, and part of the genes were annotated only in one database. Overall, there were 4.48% of the genes annotated in all of the databases, and 53.13% of the genes were annotated in at least one database.

3.3. Differential expressed genes

A total of 526 significantly differentially expressed genes (DEGs) were observed in LAV compared to LV and LA, containing 67 genes uniquely expressed in the LAV group and 270 genes uniquely expressed in the LV and LA groups. In addition, 21 and 150 genes were down-regulated and up-regulated in the LV_AV group, respectively. The global expression of the DEGs were further estimated by a hierarchical cluster analysis according to the relative expression level among LAV, LV and LA. The hierarchical clustering of the DEGs provided an intuitive way to display the clustering patterns of the DEGs among the three groups, which showed that the expression pattern of the DEGs in LAV was distinguishable from that in LV and LA (Fig. 3).

Among the 526 DEGs, 421 (78.69%) genes were annotated in the public databases. We pay more attention for the DEGs with strong homologies to the functional reported genes, so verify their function in the public reports by searching and reading their published articles.

Table 2
List of some candidate genes have homologies with reported genes.

NR Description	FPKM (LAV)	FPKM (LV)	FPKM (LA)	Reported functions
Ectropic viral integration site 2A protein (EVI2A)	**127.80**	0.18	0.00	Pathogen invasion
vitelline membrane outer layer protein I-like protein	**169.04**	0.00	0.00	Pathogen invasion
Importin-9	4.00	0.00	2.70	Pathogen invasion
Ankyrin repeat protein	**1.13**	0.00	0.24	Pathogen adhesion
oligoribonuclease	15.59	0.00	3.90	Required for pathogenesis
Adenylate cyclase associated (CAP) N terminal	**1.30**	0.25	0.00	Increase the pathogenicity
Herpesvirus latent membrane protein 1 (LMP1)	17.78	0.00	3.36	Inhibit host antiviral defense of necroptotic pathway
cathepsin C	7.27	0.50	0.13	Activate inflammatory
E3 ubiquitin-protein ligase Su(dx)	**7.92**	0.15	0.17	Protein ubiquitination
Histone methylation protein DOT1	34.06	1.22	4.75	Histone methylation
O-methyltransferase	**60.09**	0.11	0.29	Protein methylation
Apoptosis signal-regulating kinase 1	**1.49**	0.00	0.16	Pathological apoptosis
Bacteriochlorophyll A protein	**4.53**	0.00	0.00	Photosynthesis
Apolipophorins	0.00	**3.36**	**11.13**	Suppression of bacterial pathogenesis, and virus toxicity neutralization
Heterogeneous nuclear ribonucleoprotein K	0.01	**2.92**	**7.26**	Viral multiplication
Cytosol aminopeptidase family	0.00	**5.04**	**3.64**	Proteolysis against viral infections
C-type lectin	0.24	**5.02**	**2.59**	Resistant to infectious and non-infectious diseases
MHC class I antigen	0.00	**2.95**	**2.17**	Antigen processing and presentation for pathogen defense
Paramyosin	7.12	96.00	93.26	Antigen processing by positive regulation of autophagy
mRNA capping enzyme	0.00	**2.38**	**2.95**	Inhibit Protein Kinase A activity to maintain homeostasis
ATP synthase F0 subunit 6 (mitochondrion)	0.00	**3.03**	**15.44**	Antioxidant defense and oxidative damage repair
Mitochondrial proteolipid	0.00	**114.07**	**220.60**	Antioxidant defense and oxidative damage repair
NADH dehydrogenase subunit 2 (mitochondrion)	0.00	**1.04**	**4.92**	Antioxidant defense and oxidative damage repair
carboxylesterase	0.00	**21.63**	**23.03**	Positive regulation of apoptotic process for homeostasis
Bcl-2	0.00	**3.71**	**21.49**	Positive regulation of apoptotic process for homeostasis
cytochrome *b* (mitochondrion)	0.00	**1.17**	**5.46**	Positive regulation of apoptotic process for homeostasis
cytochrome *c* oxidase subunit I (mitochondrion)	0.00	**1.17**	**6.00**	Positive regulation of apoptotic process for homeostasis
Legumain-like protease precursor	0.29	**80.50**	**95.47**	Positive regulation of programmed cell death in defense responses
Rap1 GTPase-activating protein 1	0.03	**2.80**	**5.47**	Small GTPase mediated signal transduction for immune defense
Cdc42	0.00	**4.72**	**3.04**	Small GTPase mediated signal transduction for immune defense
Major Facilitator Superfamily	0.00	**1.55**	**3.50**	Protein transmembrane transport for immune defense
Translocation protein Sec62	1.07	21.24	57.41	Protein transport for immune defense
hemolymph clottable protein	0.00	**33.11**	**37.46**	Lipid transport for immune defense
T-cell immunomodulatory protein	0.22	**2.67**	**2.95**	Immune Defense
Immunoglobulin alpha heavy chain	0.00	**2.95**	**10.87**	Immune Defense
innexin 3	0.00	**4.40**	**1.55**	Immune Defense
JHE-like carboxylesterase 2	0.00	**3.64**	**2.73**	Immune Defense
Small nuclear ribonucleoprotein Sm D3	0.00	**10.48**	**41.30**	Immune Defense
Cathelicidin	0.80	15.64	4.71	Defense response
RNA recognition motif.	0.00	**7.58**	**2.12**	Stress response
Neuroglian precursor	0.00	**4.47**	**1.09**	Maintain epithelial integrity and inhibit tumor invasion
N-glycosylation protein	0.00	**3.47**	**1.48**	Protect the proteins against proteolytic degradation, and aggregation
DNA damage-regulated autophagy modulator protein 2	0.00	**7.76**	**2.34**	DNA damage repair
Gammaherpesvirus capsid protein	0.00	**3.62**	**3.97**	Regulation of transcription
Transcription initiation factor IIF, alpha subunit (TFIIF-alpha)	2.55	8.67	6.08	Regulation of transcription
Bacterial regulatory helix-turn-helix proteins, AraC family	0.00	**88.30**	**10.59**	Regulation of transcription
Eukaryotic translation initiation factor 3	0.00	**24.10**	**33.74**	Regulation of transcription
Zinc-finger of the MIZ type	0.00	**5.00**	**23.18**	Regulation of transcription
Taurine transporter	1.38	34.69	72.29	RNA-dependent DNA replication
RF-1 domain	0.00	**8.16**	**2.70**	Regulation of translational termination

FPKM, the expected number of Fragments Per Kilobase of transcript sequence per Millions base pairs sequenced. For the transcriptome analysis in the species without genome reference, it is suggested that FPKM > 0.3 represents gene is expressed. The number with bold style presents the genes uniquely expressed.

Information for the 50 DEGs that have strong homologies with reported genes were listed in Table 2, showing that 8 up-regulated DEGs (61.54%) were uniquely expressed and 32 down-regulated DEGs (86.49%) were lost expressed in the LAV group. According to the public functional reports, the up-regulated DEGs mainly involved in the fowling functions: (1) increasing pathogen adhesion and invasion; (2) necessary for pathogenesis and increasing pathogenicity; (3) inhibiting host antiviral defense; (4) activating inflammatory and pathological apoptosis; and (5) increasing protein modification (such as ubiquitination and methylation), etc. The down-regulated DEGs mainly involved in the fowling functions: (1) favoring viral multiplication; (2) inhibiting antigen processing and presentation for pathogen defense, and resistance to infectious and non-infectious diseases; (3) inhibiting antioxidant defense and oxidative damage repair, and positive regulation of apoptotic process for host homeostasis; (4) inhibiting DNA damage repair; (5) inhibiting transcription and protein transport, etc.

3.4. Functional enrichment analysis of GO and KEGG pathways

For the DEGs detected in LAV group compared to LV and LA, the main molecular functions they exercise were identified by enrichment analysis of GO and KEGG pathway. A total of 4 significantly changed GO terms (q value < 0.05) were obtained in the DEGs (Fig. 4), among which one and three terms were classified into the categories of molecular function and biological process, respectively. The changed GO terms were G-protein coupled receptor kinase activity (GO:0004703), termination of signal transduction (GO:0023,021), termination of G-protein coupled receptor signaling pathway (GO:0038,032), and negative regulation of G-protein coupled receptor protein signaling pathway (GO:0045,744).

Excepting for the replicates of unigenes that were enriched to different GO terms and after eliminating the different unigenes that assigned to the same reference gene, two genes were observed in the 4 significantly changed GO terms, which were cAMP-dependent protein

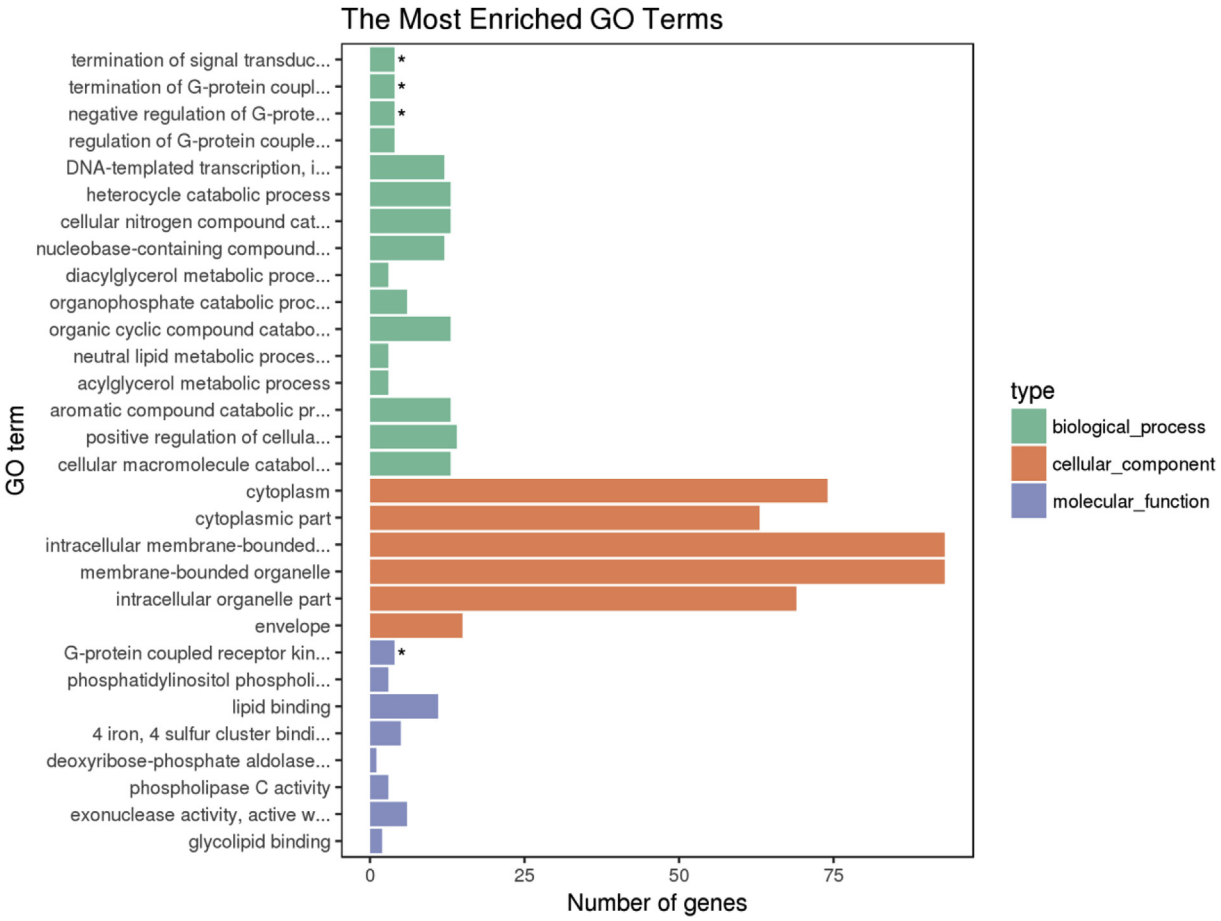

Fig. 4. The top thirty GO terms obtained in the differentially expressed genes, and * represents the significantly difference among LAV, LV and LA groups at q value < 0.05.

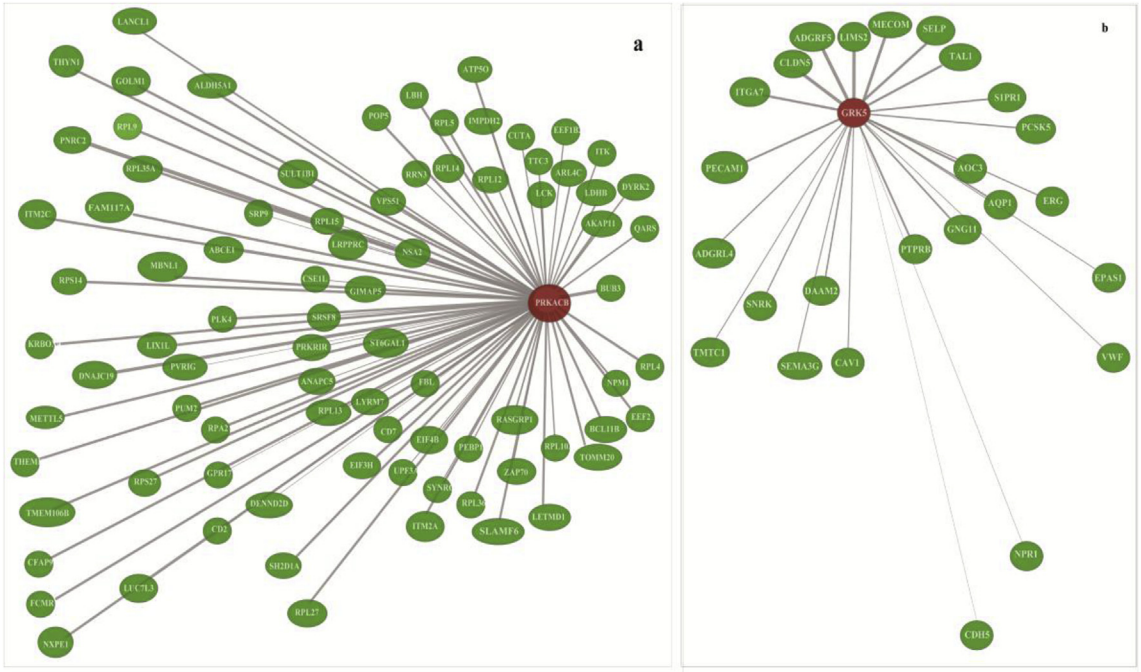

Fig. 5. The co-expression network of cAMP-dependent protein kinase catalytic subunit (PRKACB) and G protein-coupled receptor kinase (GRK) for inflammation according to the human database.

Table 3
List of the genes in significantly changed KEGG pathways.

Description (Name in pathway)	Pathway name (KO ID)
phosphoinositide 3-kinase (PI3K)	Chemokine signaling pathway (ko04062), AGE-RAGE signaling pathway in diabetic complications (ko04933)
Cdc42 (Cdc42)	Chemokine signaling pathway (ko04062), AGE-RAGE signaling pathway in diabetic complications (ko04933)
1-phosphatidylinositol 4,5-bisphosphate phosphodiesterase classes I and II (PLCβ/PLC)	Chemokine signaling pathway (ko04062), AGE-RAGE signaling pathway in diabetic complications (ko04933), African trypanosomiasis (ko05143),
G protein-coupled receptor kinase (GRK)	Chemokine signaling pathway (ko04062)
Serine/threonine-protein kinase pim (Pim-1)	AGE-RAGE signaling pathway in diabetic complications (ko04933)
immunoglobulin alpha heavy chain (IgM/IgH/IgG1/BCR)	African trypanosomiasis (ko05143), Allograft rejection (ko05330), Autoimmune thyroid disease (ko05320)
MHC class I antigen (MHC1)	Allograft rejection (ko05330), Autoimmune thyroid disease (ko05320)
apolipoprotein A-I (ApoA1)	African trypanosomiasis (ko05143), Fat digestion and absorption (ko04975)
ATP-binding cassette sub-family A member 3 (ABCA1), secretory phospholipase A2 (Lipase), Ribosomal protein L3 (FABPpm), apolipoprotein A-IV (ApoA4)	Fat digestion and absorption (ko04975)
death-associated protein kinase (DAPK), fibroblast growth factor receptor (FGFR3), interstitial collagenase (MMPs)	Bladder cancer (ko05219)
cAMP-dependent protein kinase catalytic subunit (GPRK2)	Hedgehog signaling pathway – fly (ko04341)
Beta-hexosaminidase subunit beta (3.2.1.52)	Glycosphingolipid biosynthesis-ganglio series (ko00604), Glycosaminoglycan degradation (ko00531), Glycosphingolipid biosynthesis - globo series (ko00603)
GWT1//Fungal tRNA ligase phosphodiesterase domain (2.3.1.78)	Glycosaminoglycan degradation (ko00531)
NAD+ kinase (2.7.1.23), Cytosolic purine 5′-nucleotidase (3.1.3.5), nucleoside diphosphate-linked moiety X (3.6.1.22)	Nicotinate and nicotinamide metabolism (ko00760)
Cysteine sulfinic acid decarboxylase (4.1.1.29)	Taurine and hypotaurine metabolism (ko00430)

kinase catalytic subunit (PRKACB) and G protein-coupled receptor kinase (GRK). The two genes both uniquely expressed in the LV and LA groups. The gene co-expression network of the two genes were analyzed using the Online tools Coexpedia (http://www.coexpedia.org/) according to the public human database, which showed they mainly involved in inflammation and many diseases. The overview of the co-expressed genes of PRKACB and GRK involved in inflammation were displayed in Fig. 5a and Fig. 5b, respectively.

In the enrichment analysis of KEGG pathway for the DEGs, a total of 13 significantly changed pathways were detected. After eliminating the replicates of unigenes that were enriched to different KEGG pathways and the different unigenes that assigned to the same reference gene, 22 DEGs were identified from the 13 significantly changed KEGG pathways (Table 3).

The network diagram of these KEGG pathways showed that the DEGs were at the critical nodes and were significantly down regulated in the LAV group compared to the LV and LA groups. According to the illustration of the pathways, they mainly lead to the following effects: (1) immunosuppression, anemia, endocrine dysfunction, apoptosis, blood-brain barrier penetration, neuroinvasion, circadian disturbance, neurotoxic effect, and parasite traversal (Fig. 6a); (2) apoptosis, necrosis, and thyroid disorder (Fig. 6b); (3) allograft destruction (Fig. 6c); (4) affecting angiogenesis and cell cycle (Fig. 6d); (5) cell hypertrophy, mesangial matrix expansion, angiogenesis, thrombogenesis, inflammation, atherosclerosis, apoptosis, and vascular remodeling (Fig. 6e); (6) reducing lymph transferred to blood stream (Fig. 6f); (7) cytokine production, cellular growth and differentiation, cell survival, migration, apoptosis, chemotaxis, cellular shape changes, metestasis, degranulation, ROS production, and NO induction (Fig. 6g).

3.5. Validation of RNA-seq results by real-time PCR

For the seven differentially expressed genes that were selected for validation of the Illumina sequences by real-time PCR analysis, their quantitative results were all consistent with the results of the RNA-seq technology (Fig. 7). According to their public functional reports, they were potentially involved in immune defense, apoptosis, pathogen adhesion and invasion, and protein methylation. These results confirm the reliability of RNA-seq and accuracy of the Trinity assembly, which not only verified the differential expression of the genes from the Illumina sequencing data, but also validated the reliability of the genes involved in the disease occurrence caused by ammonia toxicity. These genes would be candidates for further research.

4. Discussion

Increased ammonia in the cultured water could inhibit the immune system and increase pathogen infection severity in aquatic species [5–8], but little information was available for the mechanism of disease occurrence caused by ammonia toxicity. In the present study, comparative transcriptome analysis was performed to identify genes and pathways involved in this process, which is the first report on molecular mechanism of immunosuppression and increase pathogen infection severity from ammonia toxicity in aquatic species.

In the present study, 78.69% of the DEGs were annotated in the public databases, and we summarized their functions according to the published articles. For the significantly up-regulated DEGs in the LAV, they were necessary for pathogenesis and could increase the pathogenicity by increasing the pathogen invasion, adhesion and multiplication, inhibiting host antiviral defense of necroptotic pathway, activating inflammatory, and increasing the protein modification (such as ubiquitination and methylation), etc. Majority of the up-regulated DEGs were uniquely expressed in the LAV group, and a few examples for their functions are provided below. Ectropic viral integration site belongs to the three amino acid loop extension family of homeodomain-containing proteins, and its key roles were documented in disease formation and normal development [26]. The adenylate cyclase-associated protein (CAP) positively regulates the adenylate cyclase, and Takach and Gold [27] revealed that the CAP could increase the pathogenicity of the pathogen. Oligoribonuclease (Orn) is a 3′ to 5′ exonuclease that degrades nanoRNAs, which can serve as primers for transcription initiation at a significant fraction of promoters, and Chen et al. [28] demonstrated an essential role of Orn in the pathogenesis of *Pseudomonas aeruginosa*. Cathepsin C is a ubiquitously expressed lysosomal cysteine exopeptidase belonging to the papain family of cysteine peptidases, and its essential role is to activate the pro-inflammatory proteases, leading to tissue damage and triggering chronic inflammation [29]. Necroptosis is an alternative programmed cell death pathway that is unleashed in the absence of apoptosis, which has recently been implicated in host defense system to eliminate pathogen-infected cells. However, some viral species have evolved mechanisms (such as encoding latent membrane protein 1) inhibiting necroptosis to overcome host antiviral

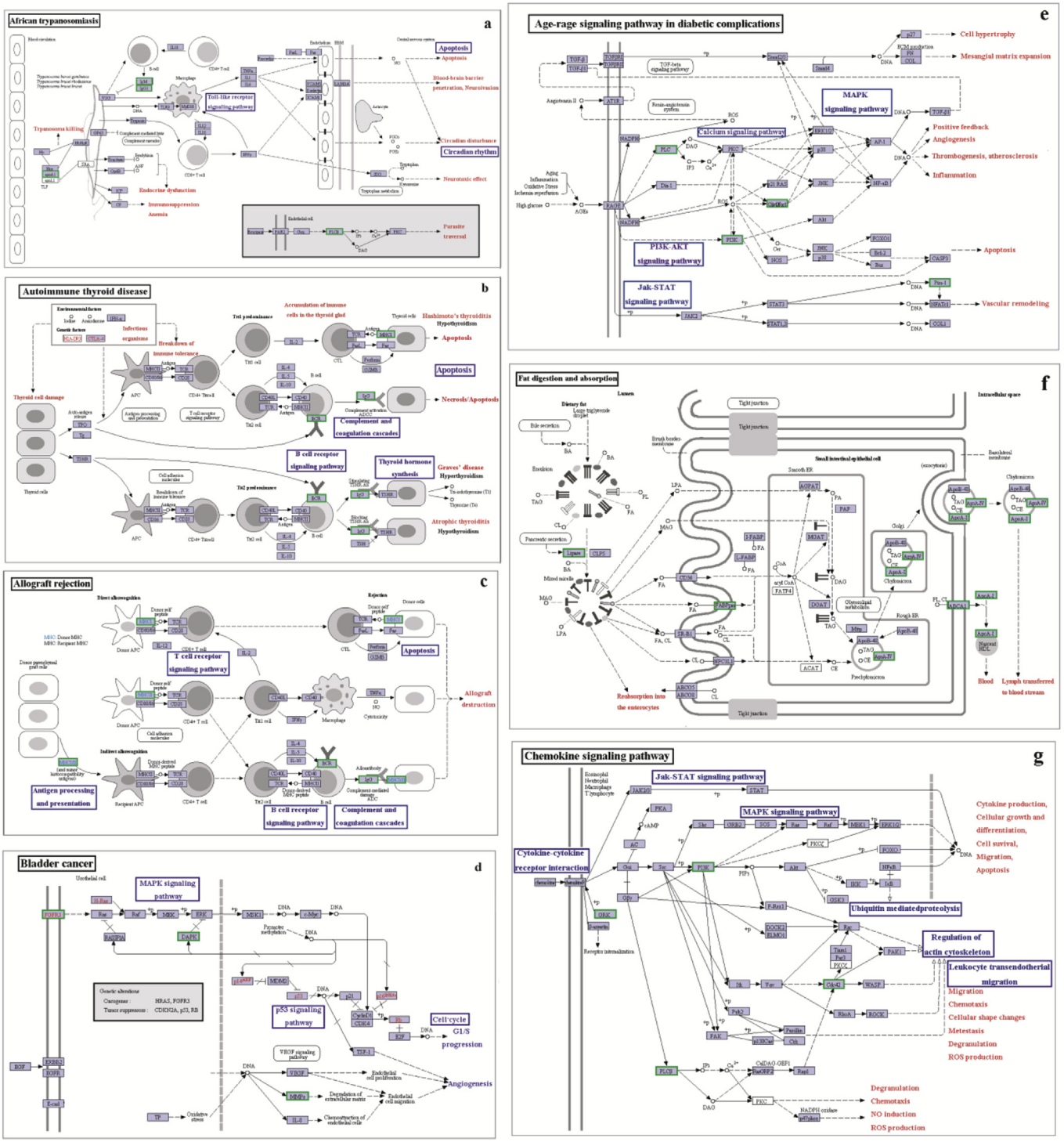

Fig. 6. The network diagrams of seven significant changed KEGG pathways. a, African trypanosomiasis; b, Autoimmune thyroid disease; c, Allograft rejection; d, Bladder cancer; e, AGE-RAGE signaling pathway in diabetic complications; f, Fat digestion and absorption; g, Chemokine signaling pathway. The green frames represents the genes were down-regulated.

defense, which is important for successful pathogenesis [30].

For the significantly down-regulated DEGs in the LAV, they would reduce the ability of suppression of bacterial pathogenesis and proteolysis against viral infections, inhibition of viral multiplication, antioxidant defense and oxidative damage repair, DNA damage repair, protein transport, and regulation of transcription, etc. Majority of the down-regulated DEGs were lost expressed in the LAV group, and a few examples for their functions are also provided below. Apolipoproteins are increasingly recognized to be functioning in the innate immune systems of animals, and it was revealed play roles in suppression of bacterial pathogenesis and virus toxicity neutralization [31]. The Hedgehog (Hh) signaling pathway is essential for tissue homeostasis in many species, and dysregulation of Hh signaling has been implicated in a large number of human disorders, but mRNA capping enzyme positively regulates Hh signaling activity to maintain homeostasis [32]. In addition, the Hh signaling pathway in the present study was also significantly down regulated (Table 3). The inhibition of protein synthesis is achieved by a reduced initiation of translation through the

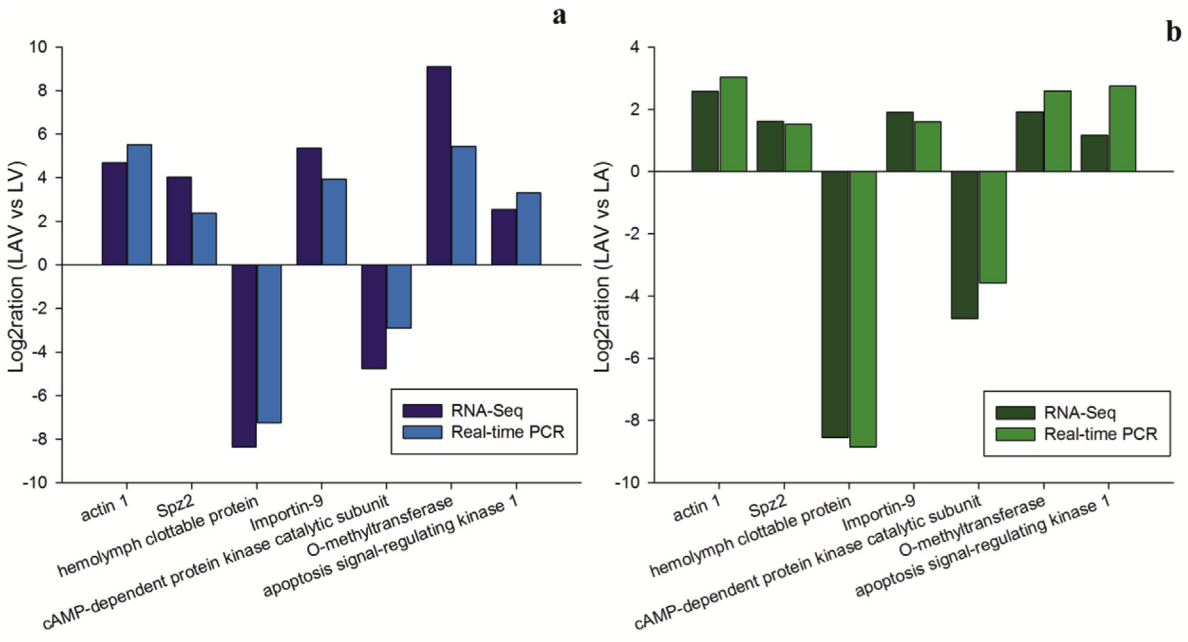

Fig. 7. Validation results of RNA-seq sequencing by real-time PCR: a, Fold change between LAV and LV groups; b, Fold change between LAV and LA groups.

inactivation of eukaryotic initiation factors [33], but some DEGs involved in regulation of transcription (such as eukaryotic translation initiation factor 3, Zinc-finger of the MIZ type, gammaherpesvirus capsid protein, and bacterial regulatory helix-turn-helix proteins, etc.) were lost expressed in the LAV group. The functions of more other DEGs could be found in Table 2.

According to the public functional reports, many of the enriched DEGs mainly involved in apoptosis process. Apoptosis plays two opposite functions in the organism, one is positive function and the other is pathological function. In the positive function, apoptosis is an essential role in animal development, homeostasis, etc. [34]. In crustacean, regulation of the intrinsic pathway of positive apoptosis represented a prerequisite to survive harsh environmental insults. Pro-apoptotic stimuli for crustaceans include UV radiation, environmental toxins, and a diatom produced chemical that promotes apoptosis in offspring of a copepod. Mechanisms that serve to depress apoptosis include the inhibition of caspase activity by high potassium in energetically healthy cells, alterations in nucleotide abundance during energy-limited states like diapause and anoxia, resistance to opening of the calcium-induced MPTP, and viral accommodation during persistent viral infection [35]. In the enriched DEGs, the important genes involved in positive apoptosis, such as Bcl-2, carboxylesterase, cytochrome *b*, cytochrome *c* oxidase subunit I, and legumain-like protease precursor [35], were lost expressed in the LAV group (Table 2), indicating that the positive regulation of apoptotic process for shrimp to survive harsh environmental insults was inhibited by ammonia stress. However, in its pathological function, apoptosis is a pivotal process in the pathogenesis of multiple diseases [36]. For example, apoptotic control lymphocyte overproduction protects against autoimmunity, but helper T cell may be programmed for suicide in a disease rather than an immune response [36]. Among the enriched DEGs, apoptosis signal-regulating kinase 1 (ASK1) involved in pathological apoptosis was uniquely expressed in the LAV group (Table 2). ASK1 is a mitogen-activated protein (MAP) kinase which activates the c-Jun N-terminal kinase (JNK) and p38 MAP kinase pathways and is required for cytokine- and stress-induced apoptosis [34], which is a pivotal component of a signaling pathway induced by many death stimuli [37].

The enrichment analysis of KEGG pathways enabled to get the functional overview for the DEGs. The network diagram showed that the DEGs were at the critical nodes of the pathways (Fig. 6), indicating they play important roles in these metabolic pathways. We paid more attention on the DEGs enriched in these KEGG pathways. The functions of some of these DEGs are provided below. According to the previous reports, GRKs (G protein-coupled receptors) widely exist in fungi, plants, invertebrates and mammals [38], which involved in many physiological processes, such as cellular metabolism, inflammatory and immune responses [39,40]. In mammals, the immune function of GRKs has been widely investigated [41,42]. In crustacean, a putative GRK was identified from red swamp crayfish (*Procambarus clarkia*), and revealed it was an important immune molecule in *P. clarkia* to defend against bacterial infection [43]. So the lost expression of GRK in LAV group might played an important role for immunosuppression by ammonia toxicity in shrimp. The IgG-like protein (immunoglobulin heavy chain) have been identified in *L. vannamei* and revealed it plays a significant role in innate defense [44], but it was lost expressed in the LAV group. Significant adhesive interactions exist between the plasma membrane and the cytoskeleton of the cells, which ensure the cells to perform their important functions, and the phosphatidylinositol-4, 5-bisphosphate 3-kinase (PI3K) as a second messenger regulates the cytoskeleton-plasma membrane adhesion [45]. However, PI3K was lost expressed in LAV group. Apolipoprotein A (ApoA) were major high density lipoprotein apoproteins, and lymph was important for protects against autoimmunity, so the lost expression of ApoA1 and ApoA4 in the LAV group inhibits the lymph transferred to blood stream for immune defense. MHC class I antigen (MHC1) present peptides at the cell surface to $CD8^+$ T cells, and plays an important role in the immune system [46]. The lost expression of MHC1 in the LAV group reduce the ability for removal of foreign bodies and apoptosis. The Cdc42 is one of the Ras-related GTP-binding proteins that control the assembly and disassembly of the actin cytoskeleton in response to extracellular signals [47]. The lost expression of Cdc42 in the LAV group reduced the functions of migration, chemotaxis, cellular shape changes, metestasis, degranulation, and ROS production. The ATP-binding cassette (ABC) superfamily of genes encode membrane proteins that transport a diverse set of substrates across membranes [48]. The lost expression of ABCA1 in the LAV group inhibits the lymph transferred to blood stream for protects against autoimmunity.

5. Conclusion

Overall, the present study represents the first analysis for molecular mechanism of immunosuppression and increasing pathogen infection severity caused by ammonia toxicity in aquatic species. The interesting founding is that among the 526 significantly differential expressed genes (DEGs), 270 DEGs were lost expressed and 67 DEGs uniquely expressed in the LAV group compared to the LV and LA groups. In addition, 13 pathways were detected to be involving in the process of immunosuppression and increasing pathogen infection severity. The involved genes and pathways could increase the pathogenicity by increasing pathogen adhesion, invasion and multiplication, inflammatory, and protein methylation and ubiquitination. In addition, they could reduce the host ability of suppression of bacterial pathogenesis and proteolysis against viral infections, antioxidant defense and oxidative damage repair, DNA damage repair, positive regulation of apoptotic for host homeostasis, protein transport and regulation of transcription, etc. The present results is a prerequisite for better understanding the molecular mechanism of disease occurrence from ammonia toxicity.

Acknowledgement

This project was financially supported by the Central Public-interest Scientific Institution Basal Research Fund, CAFS (No. 2018GH12); the National Natural Science Foundation of China (No. U1706203); Shandong province agricultural seed improvement project (No. 2017LZN011); Central Public-interest Scientific Institution Basal Research Fund, YSFRI, CAFS (No. 20603022018003); the Taishan scholar program for seed industry; and China Agriculture Research System-48.

References

[1] X. Lu, S. Luan, K. Luo, X.H. Meng, W.J. Li, J. Sui, B.X. Cao, J. Kong, Genetic analysis of the Pacific white shrimp (*Litopenaeus vannamei*): heterosis and heritability for harvest body weight, Aquacult. Res. 47 (11) (2016) 3365–3375.

[2] S.E. Peng, C.F. Lo, K.F. Liu, G.H. Kou, The transition from pre-patent to patent infection of white spot syndrome virus (WSSV) in *Penaeus monodon* triggered by pereiopod excision, Fish Pathol. 33 (4) (1998) 395–400.

[3] K.M. Alagappan, D. Deivasigamani, S.T. Somasundaram, S. Kumaran, Occurrence of *Vibrio parahaemolyticus* and its specific phages from shrimp ponds in east coast of India, Curr. Microbiol. 61 (4) (2010) 235–240.

[4] G.S. Li, J.G. He, G.F. Li, J.B. Jiang, F. Mo, Y.T. Lu, N. Lin, W.G. Peng, Relationships between *Penaeus monodon* Baculovirus Infection and Physical and Chemical Elements of Prawn-Farming Pond Water, Supplement to the journal of Sun Yatsen University, 1996, pp. 26–30 Suppl.

[5] C.H. Liu, J.C. Chen, Effect of ammonia on the immune response of white shrimp *Litopenaeus vannamei* and its susceptibility to *Vibrio alginolyticus*, Fish Shellfish Immunol. 16 (2004) 321–334.

[6] X. Lu, S. Luan, B.X. Cao, D.C. Hao, X.H. Meng, J.W. Cao, P. Dai, K. Luo, J. Kong, The investigation for the susceptibility difference of ammonia-tolerant and ammonia-sensitive populations under WSSV infection in *Litopenaeus vannamei*, Prog. Fish. Sci. 39 (1) (2018) 83–89.

[7] W. Cheng, I.S. Hsiao, J.C. Chen, Effect of ammonia on the immune response of Taiwan abalone *Haliotis diversicolor supertexta* and its susceptibility to *Vibrio parahaemolyticus*, Fish Shellfish Immunol. 17 (2004) 193–202.

[8] A. Hurvitz, H. Bercovier, J.V. Rijn, Effect of ammonia on the survival and the immune response of rainbow trout (*Oncorhynchus mykiss*, Walbaum) vaccinated against *Streptococcus iniae*, Fish Shellfish Immunol. 7 (1997) 45–53.

[9] S. Smith, L. Bernatchez, L.B. Beheregaray, RNA-seq analysis reveals extensive transcriptional plasticity to temperature stress in a freshwater fish species, BMC Genomics 14 (1) (2013) 375.

[10] J.H. Xia, P. Liu, F. Liu, G. Lin, F. Sun, R.J. Tu, et al., Analysis of stress-responsive transcriptome in the intestine of asian seabass (*Lates calcarifer*) using RNA-Se, DNA Res. 20 (2013) 449–460.

[11] J. Xu, P.F. Ji, B.S. Wang, L. Zhao, J. Wang, Z.X. Zhao, et al., Transcriptome sequencing and analysis of wild amur ide (*Leuciscus waleckii*) inhabiting an extreme alkaline-saline lake reveals insights into stress adaptation, PLoS One 8 (4) (2013) e59703.

[12] K. Chen, E.C. Li, T.Y. Li, C. Xu, X.D. Wang, H.Z. Lin, H.G. Qin, L.Q. Chen, Transcriptome and molecular pathway analysis of the hepatopancreas in the pacific white shrimp *Litopenaeus vannamei* under chronic low-salinity stress, PLoS One 10 (7) (2015) e0131503.

[13] X. Lu, J. Kong, S. Luan, P. Dai, X.H. Meng, B.X. Cao, et al., Transcriptome analysis of the hepatopancreas in the pacific white shrimp (*Litopenaeus vannamei*) under acute ammonia stress, PLoS One 11 (10) (2016) e0164396.

[14] Y. Sun, F. Li, Z. Sun, X. Zhang, S. Li, et al., Transcriptome analysis of the initial stage of acute WSSV infection caused by temperature change, PLoS One 9 (3) (2014) e90732.

[15] X.L. Shi, J. Kong, X.H. Meng, S. Luan, K. Luo, B.X. Cao N. Liu, X. Lu, K.Y. Deng, J.W. Cao, Y.X. Zhang, H.H. Zhang, X.P. Li, Comparative microarray profile of the hepatopancreas in the response of "Huanghai No. 2" *Fenneropenaeus chinensis* to white spot syndrome virus, Fish Shellfish Immunol. 58 (2016) 210–219.

[16] X. Li, X. Meng, J. Kong, K. Luo, S. Luan, B. Cao, N. Liu, J. Pang, X. Shi, Identification, cloning and characterization of an extracellular signal-regulated kinase (ERK) from Chinese shrimp, *Fenneropenaeus chinensis*, Fish Shellfish Immunol. 35 (6) (2013) 1882–1890.

[17] X. Huang, J. Chen, Y.N. Bao, L.J. Liu, H. Jiang, X. An, L.J. Dai, B. Wang, D.X. Peng, Transcript profiling reveals auxin and cytokinin signaling pathways and transcription regulation during *in vitro* organogenesis of ramie (*Boehmeria nivea* L. Gaud), PLoS One 9 (11) (2014) e113768.

[18] M.G. Grabherr, B.J. Haas, M. Yassour, J.Z. Levin, D.A. Thompson, et al., Full-length transcriptome assembly from RNA-Seq data without a reference genome, Nat. Biotechnol. 29 (2011) 644–652.

[19] J.D. Storey, R. Tibshirani, Statistical significance for genomewide studies, Proc. Natl. Acad. Sci. USA 100 (2003) 9440–9445.

[20] M.D. Young, M.J. Wakefield, G.K. Smyth, et al., Gene ontology analysis for RNA-seq: accounting for selection bias, Genome Biol. (2010), https://doi.org/10.1186/gb-2010-11-2-r14.

[21] M. Kanehisa, M. Araki, S. Goto, et al., KEGG for linking genomes to life and the environment, Nucleic Acids Res. 36 (2008) D480–D484.

[22] X. Mao, T. Cai, J.G. Olyarchuk, et al., Automated genome annotation and pathway identification using the KEGG Orthology (KO) as a controlled vocabulary, Bioinformatics 21 (2005) 3787–3793.

[23] B. Eisenhaber, P. Bork, F. Eisenhaber, Prediction of potential GPI-modification sites in proprotein sequences, J. Mol. Biol. 292 (1999) 741–758.

[24] B. Eisenhaber, P. Bork, Y. Yuan, G. Loeffler, F. Eisenhaber, Automated annotation of GPI anchor sites: case study C. elegans, Trends Biochem. Sci. 25 (2000) 340–341.

[25] Q.L. Zhang, F.H. Li, X.J. Zhang, B. Dong, J.Q. Zhang, Y. Xi, J.H. Xiang, cDNA cloning, characterization and expression analysis of the antioxidant enzyme gene, catalase, of Chinese shrimp *Fenneropenaeus chinensis*, Fish Shellfish Immun. (2008) 584–591.

[26] P. Xiang, C.Y. Lo, B. Argiropoulos, C.B. Lai, A. Rouhi, S. Imren, X.Y. Jiang, D. Mager, R.K. Humphries, Identification of E74-like factor 1 (ELF1) as a transcriptional regulator of the Hox cofactor MEIS1, Exp. Hematol. 38 (2010) 798–808.

[27] J.E. Takach, S.E. Gold, Identification and characterization of Cap1, the adenylate cyclase-associated protein (CAP) ortholog in *Ustilago maydis*, Physiol. Mol. Plant Pathol. 75 (2010) 30–37.

[28] G.K. Chen, Q. Zhao, F. Zhu, R.H. Chen, Y.X. Jin, C. Liu, X.L. Pan, S.G. Jin, W.H. Wu, Z.H. Cheng, Oligoribonuclease is required for the type III secretion system and pathogenesis of *Pseudomonas aeruginosa*, Microbiol. Res. 188–189 (2016) 90–96.

[29] B. Korkmaz, G.H. Caughey, I. Chapple, F. Gauthier, J. Hirschfeld, D.E. Jenne, R. Kettritz, G. Lalmanach, A.S. Lamort, C. Lauritzen, M. Łęgowska, A. Lesner, S. Marchand-Adama, S.J. McKaig, C. Moss, J. Pedersen, H. Roberts, A. Schreiber, S. aSeren, N.S. Thakker, Therapeutic targeting of cathepsin C: from pathophysiology to treatment, Pharmacol. Ther. 190 (2018) 202–236.

[30] X.L. Liu, Y.S. Li, S.L. Peng, X.F. Yu, W. Li, F. Shi, X.J. Luo, M. Tang, Z.Q. Tan, A.M. Bode, Y. Cao, Epstein-Barr virus encoded latent membrane protein 1 suppresses necroptosis through targeting RIPK1/3 ubiquitination, Cell Death Dis. 9 (2018) 53.

[31] D.H. Wen, H. Luo, T.N. Li, C.F. Wu, J.H. Zhang, X.L. Wang, R. Zhang, Cloning and characterization of an insect apolipoprotein (apolipophorin-II/I) involved in the host immune response of *Antheraea pernyi*, Dev. Comp. Immunol. 77 (2017) 221–228.

[32] P. Chen, Z.Z. Zhou, X. Yao, S. Pang, M.J. Liu, W.R. Jiang, J. Jiang, Q. Zhang, Capping enzyme mRNA-cap/RNGTT regulates hedgehog pathway activity by antagonizing protein kinase A, Sci. Rep. UK 7 (2017) 2891.

[33] G.C. Scheper, R. Van Wijk, A.A.M. Thomas, Regulation of the activity of eukaryotic initiation factors in stressed cells, in: R.E. Rhoads (Ed.), Signaling Pathways for Translation. Progress in Molecular and Subcellular Biology, 27. Pp3vols. 9–40 Springer, Berlin, Heidelberg, 2001.

[34] M. Saitoh, H. Nishitoh, M. Fujii, K. Takeda, K. Tobiume, Y. Sawada, M. Kawabata, K. Miyazono, H. Ichijo, Mammalian thioredoxin is a direct inhibitor of apoptosis signal-regulating kinase (ASK) 1, EMBO J. 17 (1998) 2596–2606.

[35] M.A. Menze, G. Fortner, S. Nag, S.C. Hand, Mechanisms of apoptosis in Crustacea: what conditions induce versus suppress cell death? Apoptosis 15 (2010) 293–312.

[36] J.J. Cohen, Apoptosis: the physiologic pathway of cell death, Hosp. Pract. 28 (1993) 35–43.

[37] L.X. Zhang, J. Chen, H.A. Fu, Suppression of apoptosis signal-regulating kinase 1-induced cell death by 14-3-3 proteins, Proc. Natl. Acad. Sci. Unit. States Am. 96 (15) (1999) 8511–8515.

[38] W.K. Kroeze, D.J. Sheffler, B.L. Roth, G-protein-coupled receptors at a glance, J. Cell Sci. 116 (2003) 4867–4869.

[39] A. Kohyama-Koganeya, Y.-J. Kim, M. Miura, Y. Hirabayashi, A Drosophila orphan G protein-coupled receptor BOSS functions as a glucose-responding receptor: loss of boss causes abnormal energy metabolism, Proc. Natl. Acad. Sci. U.S.A. 105 (2008) 15328–15333.

[40] T.E. Hébert, M. Bouvier, Structural and functional aspects of G protein-coupled receptor oligomerization, Biochem. Cell Biol. 76 (1998) 1–11.

[41] I. Liebscher, U. Müller, D. Teupser, E. Engemaier, K.M.Y. Engel, L. Ritscher, D. Thor,

K. Sangkuhl, A. Ricken, A. Wurm, D. Piehler, S. Schmutzler, H. Fuhrmann, F.W. Albert, A. Reichenbach, J. Thiery, T. Schöneberg, A. Schulz, Altered immune response in mice deficient for the G protein-coupled receptor GPR34, J. Biol. Chem. 286 (2011) 2101–2110.

[42] J. Zhang, L. Yang, Z. Ang, S.L. Yoong, T.T.T. Tran, G.S. Anand, N.S. Tan, B. Ho, J.L. Ding, Secreted M-ficolin anchors onto monocyte transmembrane G protein-coupled receptor 43 and cross talks with plasma C-reactive protein to mediate immune signaling and regulate host defense, J. Immunol. 185 (2010) 6899–6910.

[43] C.H. Dong, P. Zhang, A putative G protein-coupled receptor involved in innate immune defense of *Procambarus clarkii* against bacterial infection, Comp. Biochem. Physiol. Mol. Integr. Physiol. 161 (2) (2012) 95–101.

[44] Y.L. Zhang, S.Y.G. Wang, X.X. Peng, Identification of a type of human IgG-like protein in shrimp *Penaeus vannamei* by mass spectrometry, J. Exp. Mar. Biol. Ecol. 301 (2004) 39–54.

[45] D. Raucher, T. Stauffer, W. Chen, K. Shen, S.L. Guo, J.D. ork, M.P. Sheetz, T. Meyer, Phosphatidylinositol 4,5-bisphosphate functions as a second messenger that regulates cytoskeleton–plasma membrane adhesion, Cell 100 (2) (2000) 221–228.

[46] J. Neefjes, M.L.M. Jongsma, P. Paul, O. Bakke, Towards a systems understanding of MHC class I and MHC class II antigen presentation, Nat. Rev. Immunol. 11 (2011) 823–836.

[47] Nicolas Tapon Alan Hall, Rho, Rac and Cdc42 GTPases regulate the organization of the actin cytoskeleton, Curr. Opin. Cell Biol. 9 (1) (1997) 86–92.

[48] M. Dean, T. Annilo, Evolution of the ATP-binging cassette (ABC) transporter superfamily in vertebrates, Annu. Rev. Genom. Hum. Genet. 6 (2005) 123–142.